



**HAL**  
open science

## Passage of uranium through human cerebral microvascular endothelial cells: influence of time exposure in mono- and co-culture in vitro models

Celine Gloaguen, Ana F Raimundo, Christelle Elie, Alain Schmitt, Magali Floriani, Séverine Favard, Denis Monneret, F Imbert-Bismut, Nicolas Weiss, Maria A Deli, et al.

### ► To cite this version:

Celine Gloaguen, Ana F Raimundo, Christelle Elie, Alain Schmitt, Magali Floriani, et al.. Passage of uranium through human cerebral microvascular endothelial cells: influence of time exposure in mono- and co-culture in vitro models. *International Journal of Radiation Biology*, 2020, 96 (12), pp.1597-1607. 10.1080/09553002.2020.1828655 . hal-03080771v2

HAL Id: hal-03080771

<https://hal.science/hal-03080771v2>

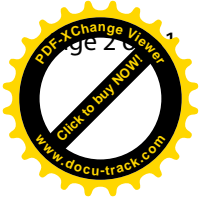
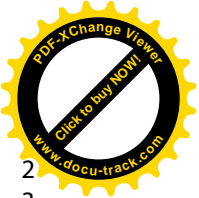
Submitted on 1 Aug 2023

**HAL** is a multi-disciplinary open access archive for the deposit and dissemination of scientific research documents, whether they are published or not. The documents may come from teaching and research institutions in France or abroad, or from public or private research centers.

L'archive ouverte pluridisciplinaire **HAL**, est destinée au dépôt et à la diffusion de documents scientifiques de niveau recherche, publiés ou non, émanant des établissements d'enseignement et de recherche français ou étrangers, des laboratoires publics ou privés.



Distributed under a Creative Commons Attribution - NonCommercial 4.0 International License



2  
3  
4 1 **PASSAGE OF URANIUM THROUGH HUMAN CEREBRAL**  
5  
6 2 **MICROVASCULAR ENDOTHELIAL CELLS: INFLUENCE OF TIME**  
7  
8  
9 3 **EXPOSURE IN MONO- AND CO-CULTURE *IN VITRO* MODELS.**

4 **C. Gloaguen<sup>1S</sup>, A.F. Raimundo<sup>1S</sup>, C. Elie<sup>1</sup>, A. Schmitt<sup>2</sup>, M. Floriani<sup>3</sup>, S. Favard<sup>4</sup>, D. Monneret<sup>4</sup>, F.**  
5 **Imbert-Bismut<sup>4</sup>, N. Weiss<sup>5,6</sup>, M.A. Deli<sup>7</sup>, K. Tack<sup>1</sup>, P. Lestaevel<sup>1\*</sup>, M. A. Benadjaoud<sup>1</sup> and A.**  
6 **Legendre<sup>1</sup>.**

7 <sup>1</sup>Institut de Radioprotection et Sûreté Nucléaire (IRSN), PSE-SANTE/SESANE/LRTOX, PSE-SANTE/SERAMED,  
8 Fontenay aux Roses, 92262 , France

9 <sup>2</sup> Electronic Microscopy Facility, INSERM UMR 1016, Cochin Institute, Paris, France

10 <sup>3</sup> Institut de Radioprotection et Sûreté Nucléaire (IRSN), PSE-ENV/SRTE/LECO Saint Paul Lez Durance, 13115, France

11 <sup>4</sup> Department of Metabolic Biochemistry, La Pitié- Salpêtrière- Charles Foix University Hospital (APHP), Paris, France

12 <sup>5</sup> Sorbonne Université, Brain Liver Pitié-Salpêtrière (BLIPS) Study Group, INSERM, Centre de Recherche Saint-Antoine,  
13 Assistance Publique - Hôpitaux de Paris, Groupement Hospitalier Pitié-Salpêtrière Charles Foix, Département de Neurologie,  
14 Unité de réanimation neurologique, Paris, France

15 <sup>6</sup> Unité de réanimation neurologique, Pôle des Maladies du Système Nerveux, Groupe Hospitalier Pitié-Salpêtrière Charles  
16 Foix, Assistance Publique – Hôpitaux de Paris, et Institut de Neurosciences Translationnelles IHU-A-ICM, Paris, France.

17 <sup>7</sup> Institute of Biophysics, Biological Research Centre, Hungarian Academy of Sciences, Szeged, Hungary

18  
19 \*corresponding author: [philippe.lestaevel@irsn.fr](mailto:philippe.lestaevel@irsn.fr)

20 \$ equal contribution

21 **Running title: blood-brain barrier and passage of uranium**

22  
23 **Emails of authors:**

24 C. Gloaguen: [celine.gloaguen@irsn.fr](mailto:celine.gloaguen@irsn.fr)

25 A.F. Raimundo: [anafmraimundo@gmail.com](mailto:anafmraimundo@gmail.com)

26 C. Elie: [christelle.elie@irsn.fr](mailto:christelle.elie@irsn.fr)

27 A. Schmitt: [alain.schmitt@inserm.fr](mailto:alain.schmitt@inserm.fr)

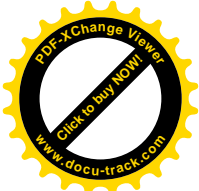
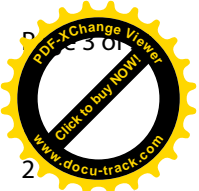
28 M. Floriani : [magali.floriani@irsn.fr](mailto:magali.floriani@irsn.fr)

29 S. Favard: [severine.favard@aphp.fr](mailto:severine.favard@aphp.fr)

30 D. Monneret: [dmonneret2@gmail.com](mailto:dmonneret2@gmail.com)

31 F. Imbert-Bismut: [francoise.bismut@aphp.fr](mailto:francoise.bismut@aphp.fr)

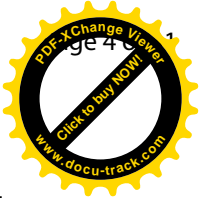
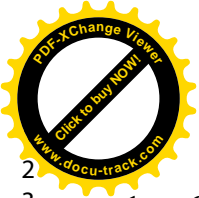
32 N. Weiss: [nicolas.weiss@aphp.fr](mailto:nicolas.weiss@aphp.fr)



2  
3  
4  
5  
6  
7  
8  
9  
10  
11  
12  
13  
14  
15  
16  
17  
18  
19  
20  
21  
22  
23  
24  
25  
26  
27  
28  
29  
30  
31  
32  
33  
34  
35  
36  
37  
38  
39  
40  
41  
42  
43  
44  
45  
46  
47  
48  
49  
50  
51  
52  
53  
54  
55  
56  
57  
58  
59  
60

- 1 M.A. Deli: [deli.maria@brc.mta.hu](mailto:deli.maria@brc.mta.hu)
- 2 K. Tack: [karine.tack@irsn.fr](mailto:karine.tack@irsn.fr)
- 3 P. Lestaevel: [philippe.lestaevel@irsn.fr](mailto:philippe.lestaevel@irsn.fr)
- 4 M. A. Benadjaoud : [mohamedamine.benadjaoud@irsn.fr](mailto:mohamedamine.benadjaoud@irsn.fr)
- 5 A. Legendre: [audrey.legendre@irsn.fr](mailto:audrey.legendre@irsn.fr)

For Peer Review Only



1 C. Gloaguen, A.F. Raimundo, C. Elie, A. Schmitt, M. Floriani, S. Favard, D. Monneret, F.  
2  
3  
4  
5 2 Imbert-Bismut, N. Weiss, M.A. Deli, K. Tack, P. Lestaevel, M. A. Benadjaoud and A. Legendre.  
6  
7

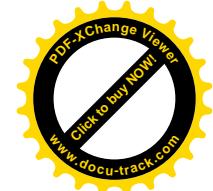
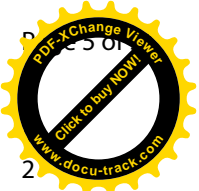
8  
9 3 **PASSAGE OF URANIUM THROUGH HUMAN CEREBRAL**  
10  
11 4 **MICROVASCULAR ENDOTHELIAL CELLS: INFLUENCE OF TIME**  
12  
13  
14 5 **EXPOSURE IN MONO- AND CO-CULTURE MODELS.**  
15  
16

17  
18 6 **ABSTRACT:**

19  
20  
21 7 Purpose: Depleted uranium (DU) has several civilian and military applications. The effects of this  
22  
23 8 emerging environmental pollutant on human health raise some concerns. Previous experimental  
24  
25 9 studies have shown that uranium (U) exposure can disturb the central nervous system. A small  
26  
27 10 quantity of U reaches the brain *via* the blood, but the effects on the blood-brain barrier (BBB) remain  
28  
29 11 unclear.

30  
31  
32 12 Materials and Methods: In the present work, two cell culture models were exposed to DU for different  
33  
34 13 times to study its cytotoxicity, paracellular permeability and extracellular concentration of U. The  
35  
36 14 well-known immortalized human cerebral microvascular endothelial cells, hCMEC/D3, were cultured  
37  
38 15 on the filter in the first model. In the second model, human primary cells of pericytes were cultured  
39  
40 16 under the filter to understand the influence of cell environment after U exposure.

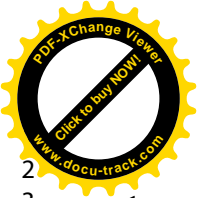
41  
42  
43 17 Results: The results show that U is not cytotoxic to hCMEC/D3 cells or pericytes until 500  $\mu\text{M}$   
44  
45 18 ( $1.6\text{Bq}\cdot\text{L}^{-1}$ ). In addition, acute or chronic low-dose exposure of U did not disturb permeability and was  
46  
47 19 conserved in both cell culture models. However, U is able to reach the brain compartment. During the  
48  
49 20 first hours of exposure, the passage of U to the abluminal compartment was significantly reduced in  
50  
51 21 the presence of pericytes. Electronic microscopy studies evidenced the formation of needle-like  
52  
53 22 structures, like urchin-shaped precipitates, from 1 h of exposure. Analytical microscopy confirmed the  
54  
55 23 U composition of these precipitates. Interestingly, precipitated U was detected only in endothelial cells  
56  
57 24 and not in pericytes. U was localized in multilamellar or multivesicular bodies along the endo-  
58  
59  
60



1 lysosomal pathway, suggesting the involvement of these traffic vesicles in U sequestration and/or  
2  
3  
4  
5 2 elimination.

6  
7  
8 3 Conclusions: We show for the first time the *in vitro* passage of U across a human cerebral  
9  
10 4 microvascular endothelial cells, and the intracellular localization of U precipitates without any  
11  
12 5 cytotoxicity or modification of paracellular permeability. The difference between the results obtained  
13  
14 6 with monolayers and co-culture models with pericytes illustrates the need to use complex *in vitro*  
15  
16 7 models in order to mimic the neurovascular unit. Further *in vivo* studies should be performed to better  
17  
18 8 understand the passage of U across the blood-brain barrier potentially involved in behavioral  
19  
20 9 consequences.

21  
22  
23  
24 10 Keywords: pericytes; human endothelial cell; uranium; permeability.  
25  
26  
27  
28  
29  
30  
31  
32  
33  
34  
35  
36  
37  
38  
39  
40  
41  
42  
43  
44  
45  
46  
47  
48  
49  
50  
51  
52  
53  
54  
55  
56  
57  
58  
59  
60

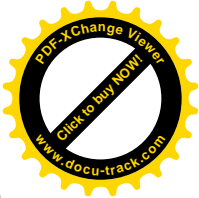


1

## 2 INTRODUCTION:

3 Uranium (U) is a heavy metal and radionuclide that is found naturally in the Earth's crust, and so is  
4 also present in underground water, air, plants and animals. In addition, certain human activities,  
5 industrial, nuclear or military, lead to the production of U waste, which increases the risk of human  
6 low-dose exposure. This waste is mainly composed of depleted uranium (DU) and is now considered  
7 an emerging environmental pollutant (Faa et al. 2018). DU contains a low level of  $^{235}\text{U}$  and is around  
8 40% less radioactive than naturally occurring U. Health risk concerns have been raised for populations  
9 exposed to U, especially regarding toxicity in the kidney and central nervous system (CNS). Previous  
10 studies have shown that U ingestion affects animal behavior: impairment of locomotor activity and  
11 learning processes and increased anxiety (Briner and Murray 2005; Lestaevel et al. 2015). In fact, after  
12 ingestion of DU-contaminated drinking water ( $40 \text{ mg.L}^{-1}$ ), there were even traces of U (quantity < 3  
13 ng/L) in the brain of exposed animals and U was detected in specific brain areas - the striatum, the  
14 cortex and the hippocampus (Houpert et al. 2007). This localization of U is heterogeneous and, dose  
15 and exposition mode-dependent (Houpert et al. 2005; Tournier et al. 2009).

16 These animal data strongly suggest that radionuclide circulating in the blood could reach the brain  
17 after U exposure. Nevertheless, the brain is protected from harmful circulating compounds and  
18 xenobiotics by a unique specialized barrier, the blood-brain barrier (BBB). This barrier constitutes a  
19 specialized physical, metabolic and immunological barrier that represents the largest surface area of  
20 exchange between the blood and the brain. The BBB is localized at the level of the cerebral  
21 microvessels and is dependent on the expression of tight junctions (TJ) by cerebral endothelial cells.  
22 The permeability of these cells is highly controlled (Weiss et al. 2009; Obermeier et al. 2013). The  
23 cerebral endothelial cells lying on the basal lamina interact closely with other cell types such pericytes,  
24 glial cells, astrocytes, and neurons. All these cells together constitute the functional and organic unit  
25 that protects the brain and ensures its best functioning: the neurovascular unit (NVU) (Liebner et al.  
26 2011) . Therefore, in order to study the permeability of any agent in the CNS, it is more reliable to use



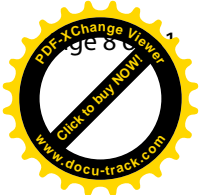
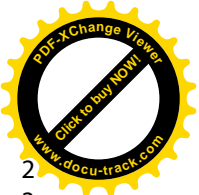
1 not only brain endothelial cells as the simplest model of the BBB, but a more complex model with  
2 other cells. The role of the BBB after U exposure remains unexplored. There is only one study  
3 showing a possible vascular transfer of U after rat brain perfusion, but without impairment of BBB  
4 integrity (Lemercier et al. 2003). In fact, one *in vitro* study on rat brain endothelial cells (RBE4 cells)  
5 evidenced no toxicity of U, despite the intracellular presence of U (Dobson A et al. 2006). Human  
6 studies on BBB transfer of U are lacking and *in vitro* models represent a great opportunity to fill the  
7 gap.

8 The aim of this work was to create a human *in vitro* model to study the effects of U exposure. The first  
9 step was to use only endothelial cells to form the BBB model. Human cerebral microvessel endothelial  
10 cells (hCMEC/D3), an immortalized line derived from human temporal lobe microvessels, was  
11 selected since in order to study the BBB *in vitro* it is more reliable model, widely used and well  
12 characterized in the literature (Weksler BB et al. 2005; Weksler B et al. 2013). The culture was static,  
13 using a Boyden-like chamber and composed of two compartments. The luminal compartment  
14 represented the blood side and the abluminal the cerebral side of the BBB thus mimicking the  
15 physiological situation. A second model was developed with human pericytes cultivated under the  
16 filter in order to reproduce the cell environment of the BBB. The objectives were to determine if U  
17 was cytotoxic for human cerebral endothelial cells and pericytes, and to study the influence of time of  
18 exposure in mono- and co-culture models on BBB permeability, the extracellular concentration of U  
19 and the intracellular localization of U.

## 22 **MATERIAL & METHODS:**

### 24 ***1. Cell culture***

#### 25 i. hCMEC/D3 cell line



1 The human cerebral microvascular endothelial cell (hCMEC/D3) line was obtained from the  
2  
3 Institut Cochin after a Mutual Transfer Agreement (LS12102) with the IRSN. They were stored at -  
4  
5 150 °C in freezing medium (95% serum and 5% dimethylsulfoxide). In the present study, the  
6  
7 hCMEC/D3 cells were used between passages 27 and 35. After thawing, the cells were seeded in T-75  
8  
9 cm<sup>2</sup> flasks, previously coated with collagen-I (Trevigen, Inc., Gaithersburg, MD, USA) from rat tail  
10  
11 tendons, dissolved in distilled water (Life Technologies, Thermo Fisher Scientific, Waltham, MA,  
12  
13 USA) at 150 µg.mL<sup>-1</sup>. Cells in T-flasks were kept in an incubator with a humidified atmosphere with  
14  
15 5% CO<sub>2</sub> at 37 °C, for 3-4 days.  
16  
17

#### 18 ii. Human Brain Vascular Pericytes

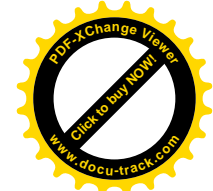
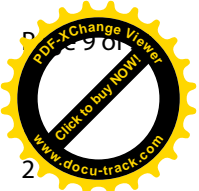
19  
20 The human brain vascular pericytes (HBVP) were from ScienCell Research Laboratories  
21  
22 (ScienCell, San Diego, CA, USA). One vial containing 5x10<sup>5</sup> cells in 1 mL was seeded in one poly-D-  
23  
24 lysine coated T-75 cm<sup>2</sup> flask, with the same medium previously used for hCMED/D3 cells.  
25  
26

27  
28 When the human endothelial cells and pericytes reached confluence, the cells were counted  
29  
30 after trypsinization using a hemocytometer (Malassez, Preciss France) and seeded at the necessary  
31  
32 concentration on other collagen-I coated supports.  
33  
34  
35

#### 36 iii. Model setup

37  
38 Two *in vitro* models of culture were established. The first was comprised only the hCMEC/D3  
39  
40 cell line (model A) and the second was a co-culture of hCMEC/D3 cells with HBVP (model B).  
41  
42 Transwells of 6- or 12-well format (24 mm or 12 mm diameter, respectively), polyester membrane, 0.4  
43  
44 µm of pore diameter (Corning, NY, USA), were coated with collagen-I from rat tail tendons  
45  
46 (Trevigen, Inc., Gaithersburg, MD, USA) at 150 µg.mL<sup>-1</sup>. The hCMEC/D3 cells were then seeded at  
47  
48 day (D) 0 on the insert at a 50000 cells/cm<sup>2</sup> concentration and kept in the incubator. The medium was  
49  
50 changed at D3, in both the luminal and abluminal compartments, and cultures were used for  
51  
52 experiments at D6. EndoGRO™ Basal Medium (EMD Millipore Corp.) supplemented with  
53  
54 EndoGRO™-MV Supplement Kit, Penicillin-Streptomycin at 10.000 U.mL<sup>-1</sup> (Life Technologies,  
55  
56  
57  
58  
59  
60





1 Thermo Fisher Scientific, Waltham, MA, USA) and HEPES 1M (Life Technologies, Thermo Fisher  
2 Scientific, Waltham, MA, USA) was used. All cultures were done with the same media.

3 To create a “close-contact” co-culture system between the hCMEC/D3 cells and HBVP  
4 (model B), pericytes were added on the day before the seeding (D-1) of the hCMEC/D3 cells on the  
5 apical side of the filter precoated with collagen-I ( $150 \mu\text{g}\cdot\text{mL}^{-1}$ ). The pericytes were seeded at a 50000  
6 cells/cm<sup>2</sup> concentration on the bottom side of the filter and the inserts were kept inverted inside a Petri  
7 dish, in the incubator, until the next day. At D0, the inserts were returned into the right position inside  
8 the well. The cell culture medium used (i.e. EngoGro Basal Medium supplemented) was the same each  
9 side of the filter.

## 11 2. Uranium exposure

12 Whatever the speciation, after exposure, U is the uranyl ion in the formal oxidation state +VI  
13  $[\text{U}(\text{VI})\text{O}_2^{2+}]$  in aqueous media. In the body, U forms complexes with citrate, bicarbonate, or proteins in  
14 the plasma (Keith et al. 2013). In order to mimic that, the U utilized for *in vitro* experiments was in the  
15 form of uranyl nitrate hexahydrate, after the reaction with bicarbonate solution. A range of  
16 experimental concentrations (50 pM to 500  $\mu\text{M}$ ) was used to test every possible effect of U in the  
17 BBB, even if the highest concentrations (above 100  $\mu\text{M}$ ) were unlikely to be attained *in vivo* (Jiang et  
18 al. 2007). These values could be compared to the concentration of uranium in biofluids after human  
19 exposure. In the blood, uranium concentrations are in the order to 0.02 nM up to 0.4 nM (Dang and  
20 Pullat 1993). These concentrations measured in human blood are several orders of magnitude below  
21 the first concentrations used in the present study

22 A 10 mM stock solution was prepared by dissolving the DU powder (ORANO, France) in 100 mM  
23  $\text{NaHCO}_3$  solution. DU has a physical half-life of 4.5 billion years and the radioactive specific activity  
24 of DU was  $1.4 \times 10^4 \text{ Bq}\cdot\text{g}^{-1}$ , and its isotopic composition was  $^{238}\text{U} = 99.74\%$ ,  $^{235}\text{U} = 0.255\%$ , and  $^{234}\text{U} =$   
25  $0.0055\%$  (pH = 7.4). DU solutions used for experiments were extemporaneously prepared by dilution  
26 of the stock solution in cell culture medium.



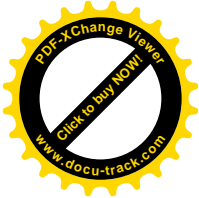
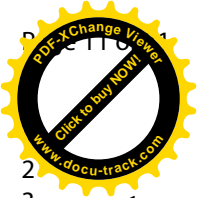
1 Different U exposure durations were performed to mimic both acute and chronic exposures when the  
2  
3 human endothelial cells and pericytes reached confluence. As the status of the cells at the time of  
4  
5 exposure can influence the cell responses, all exposures were realized on confluent cells to obtain the  
6  
7 monolayer of endothelial cells. The acute exposure was reproduced with 24, 4 and 1 hour of exposure  
8  
9 before the experiment. As for the chronic exposure, it was performed in the last 3 days of the 6 days of  
10  
11 experiment (D3D6). All these conditions are summarized in **Figure 1**.  
12  
13  
14  
15  
16  
17  
18

### 19 3. *U cytotoxicity assays*

20  
21  
22 A cell proliferation Kit I (MTT) from Roche (Cat. No. 11 465 007 001) was used to assay the cell's  
23  
24 viability and proliferation. Cells were seeded on 96-well plates coated with collagen-I at 50000  
25  
26 cells/cm<sup>2</sup> concentration. U was added to the medium at different concentrations, from 50 pM to 500  
27  
28 μM, and kept in the incubator. On the day after the seeding, the yellow 3-(4,5-dimethylthiazol-2-yl)-  
29  
30 2,5-diphenyltetrazolium bromide (MTT) salt was added to each well and, 4 hours later, the  
31  
32 solubilization agent was also added to each well. Each condition was done in sextuplicate. The  
33  
34 reaction occurred overnight in the incubator, allowing the evaluation of the plate on the next day with a  
35  
36 microplate reader at 570 nm. In order to analyze the results, the mean absorbance value measured for  
37  
38 only the medium, without cells, was subtracted from all the conditions, to remove the background  
39  
40 noise. Afterwards, the absorbance of control cell samples was considered as 100% and all the test  
41  
42 conditions were represented as percentages of the control.  
43  
44  
45  
46  
47  
48  
49

### 50 4. *Paracellular permeability assay*

51  
52 Paracellular permeability through the hCMEC/D3 monolayer was measured at D6 in 6- or 12-well  
53  
54 plates as already described (Weksler BB et al. 2005). At the time of analysis, the luminal content of  
55  
56 the inserts was removed; they were transferred into new 6- or 12-well plates containing transport  
57  
58 buffer (HBSS with 10 mM of HEPES and 1 mM of sodium pyruvate, Invitrogen) in the lower  
59  
60



1 chamber. In the upper chamber, 50  $\mu\text{M}$  Lucifer Yellow dilithium salt (LY) in transport buffer was  
 2 added and incubated at 37°C 5%  $\text{CO}_2$ . For the positive control, cells were subjected to 1.4 M of  
 3 mannitol 30 minutes before the experiment. For the negative control, cells were unexposed to U and  
 4 only 100 mM  $\text{NaHCO}_3$  solution was added. To quantify the LY passage, the abluminal compartment  
 5 was analyzed at each time point (10, 25, 45 min) using a microplate reader, with an excitation filter of  
 6 485 nm and an emission filter of 535 nm. Paracellular permeability was calculated using the clearance  
 7 principle, as described by Siflinger-Birnboim and colleagues (Siflinger-Birnboim et al. 1987). The  
 8 clearance was calculated for the coated insert without cells, called  $\text{PS}_f$ , and for each coated insert with  
 9 cells, called  $\text{PS}_t$ , each with  $\text{mL}\cdot\text{min}^{-1}$  dimensions. By using these values it was possible to obtain one  
 10 other parameter,  $\text{PSe}$ , by applying the formula:

$$\frac{1}{\text{PSe}} = \frac{1}{\text{PS}_t} - \frac{1}{\text{PS}_f}$$

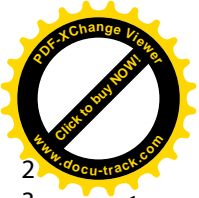
11  
 12 Finally,  $\text{PSe}$  was divided by the surface area of the filter to give the endothelial permeability  
 13 coefficient ( $\text{Pe}$ ) in  $10^{-3}$  cm/min or as the percentage of permeability normalized to the permeability  
 14 coefficient for the control conditions of untreated cells. Each condition was tested in triplicate in order  
 15 to evaluate statistical significance of these data.

16

### 17 **5. Transmission Electronic Microscopy (TEM)**

18 The cells were fixed at 2.5% glutaraldehyde in PBS [-][-], for 1 h at room temperature (RT.) Then, the  
 19 cells were postosmicated with osmium tetroxide and carefully washed in buffer before inclusion in  
 20 EPON resin. At this point, the samples were cut to the desired thickness (100nm) using an  
 21 ultramicrotome. Uranyl acetate and lead citrate were not used to contrast grids in order to avoid false  
 22 positives with U. Ultrathin sections were examined in a JEOL 1011 electron microscope equipped  
 23 with Orius 1000 camera.

24



## 6. Analytical microscopy

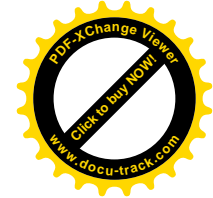
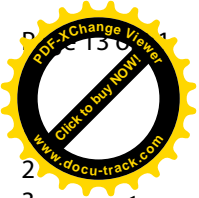
For chemical analysis, the ultrathin sections were examined with a Scanning Transmission Electron Microscope (TEM/STEM Tecnai12 G2 Biotwin Electron Microscope, FEI company of ThermoFisher scientific group) using an accelerating voltage of 100 kV and equipped with a CCD camera Megaview III (Olympus Soft imaging Solutions GmbH). Several subcellular structures were analyzed with the Energy Dispersive X-ray analyzer (EDX) equipped with a Super Ultrathin Window (SUTW) model sapphire (EDAX). Accumulation of U was detected by focusing the electron beam (20nm diameter) on specific precipitates and spectra were collected for 100 seconds.

## 7. ICP-MS evaluation of cellular and extracellular luminal and abluminal U concentrations

First, to identify the ability of U to enter each type of cell and to quantify the intracellular U content, a monoculture of hCMEC/D3 cells or pericytes was performed in the bottom of 6-well plates coated with collagen-I at 25000 cells/cm<sup>2</sup>. After seeding, cells were exposed to U during 24 h. The tested U concentrations were 1  $\mu$ M, 10  $\mu$ M, 50  $\mu$ M, 100  $\mu$ M and 250  $\mu$ M. After exposure, the cells were washed repeatedly with PBS [-] [-] supplemented with Bovine Serum Albumin 0.2% and then collected after trypsinization with 200  $\mu$ L of 69% nitric acid (Aristar quality grade, VWR Prolabo).

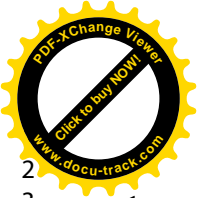
Second, to identify U passage across the BBB (*i.e.* hCMEC/D3 cell line) U content in the extracellular compartments (*i.e.* luminal and abluminal) was quantified. After the U exposure in mono- and co-culture models (in 6-well formats – see section 2. Uranium exposure), the culture medium was removed and stored at 4°C.

The duplicated or triplicated samples were diluted with 2% nitric acid. As previously described (Gueguen et al. 2015), U was quantified by Inductively-Coupled Plasma Mass Spectrometry (ICP-MS) (ICP-MS, X series II, Thermo Electron, France) using a 7700X series (Agilent Technologies, Les Ulis, France), calibrated with a SPEX CertiPrep U standard solution (Jobin Yvon, Longjumeau, France). The results of the analysis were expressed as parts per trillion (1 ppt = 1 ng.L<sup>-1</sup>).



## 8. Statistical Analysis

All results were expressed as mean  $\pm$  standard deviation (SD) from at least three independent experiments, each one performed in triplicate for each tested condition, unless stated otherwise. The significance of variability between the results from various groups was determined by one-way ANOVA when the normality assumption was met, and the Kruskal–Wallis test if not. Post-test analysis was verified by Dunn’s test. This analysis was performed using the SigmaPlot 11.0 software. The results were considered statistically different when  $p < 0.05$ . The association between LY permeability and U concentration was analyzed by a generalized estimating equation (GEE) regression (Zeger and Liang 1986) and conducted using the Zelig Package of R software (R Software 2016). The associated symbols are \* for  $p < 0.05$ , \*\* for  $p < 0.005$  and \*\*\* for  $p < 0.001$ .



## **RESULTS:**

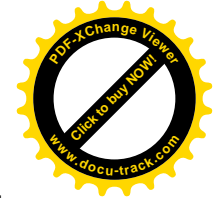
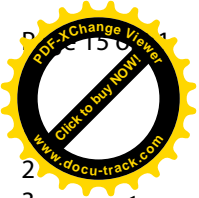
### **1. U Cytotoxicity**

Cytotoxicity tests showed no noteworthy difference between the viability of the control and of the cells subjected to concentrations up to 500  $\mu\text{M}$  of U (**Figure 2** **Error! Reference source not found.**). Even if a tendency to decreased cell viability was notable for the 250  $\mu\text{M}$  conditions, there was a statistically significant decrease on the percentage of living cells (of about 50% for each type of cell) only for 500  $\mu\text{M}$  ( $p < 0,001$ ), *i.e.* hCMEC/D3 cell line or pericytes.

### **2. U effect on *in vitro* paracellular BBB permeability**

BBB properties were evaluated after exposure of the *in vitro* model composed of hCMEC/D3 monolayer to different concentrations of U. Paracellular permeability ( $P_e$ ) to LY was studied by adding U at concentrations from 1 to 500  $\mu\text{M}$  during the permeability test (**Figure 3**). Mannitol was used as a positive control to induce osmotic shock, and therefore the disarrangement of the cells and the disruption of the TJ, which interferes with the barrier properties of the monolayer. In comparison with the negative control, LY permeability increased by a factor of three ( $1.31 \pm 0.19 \times 10^{-3} \text{ cm.min}^{-1}$  and  $3.71 \pm 1.25 \times 10^{-3} \text{ cm.min}^{-1}$ , respectively). During U exposure, paracellular permeability of the hCMEC/D3 monolayer was not affected, since the permeability remained unchanged in every condition when compared to the negative control.

In order to determine if the duration of U exposure had an effect on the paracellular permeability of the BBB, the hCMEC/D3 monolayer alone (model A) and co-cultured with pericytes (model B) were subjected to a non-cytotoxic concentration of U (50  $\mu\text{M}$ ) for different times. Several time windows of exposure of the model were defined in order to mimic acute (1, 4 and 24 h) and chronic exposures (D3D6) as described in **Figure 1**. After 6 days, LY permeability was evaluated to verify possible



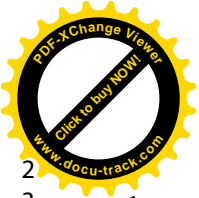
1 modifications of BBB properties. The comparison between models A and B determined whether the  
2 presence of pericytes modified the response obtained with the hCMEC/D3 monolayer alone.  
3 Control permeability value for models A and B was  $0.96 \times 10^{-3} \text{ cm.min}^{-1}$  and  $1.37 \times 10^{-3} \text{ cm.min}^{-1}$ ,  
4 respectively (**Figure 4**). This difference was statistically significant ( $p = 0.009$ ) suggesting that the co-  
5 culture with pericytes affected the BBB permeability of the hCMEC/D3 monolayer when exposed to  
6 U. Comparing each time of U exposure to its control in model A or B, the results showed no  
7 detectable statistical difference between the groups (**Figure 5**). This indicates that neither acute nor  
8 chronic exposure to U seems to affect the permeability of the monolayer in each model. Interestingly,  
9 when all parameters were taken into consideration (models A and B, passage of cells and format of  
10 wells), the results of the comparison were altered. Model A, passage 34 for the hCMEC/D3 cells (*i.e.*  
11 the most used passage), 6-w format, was considered and showed a statistical difference between the  
12 data obtained with the 6- and 12-well formats ( $p = 1.5 \times 10^{-5}$ ) by the GEE analysis. This occurred  
13 because the Pe was reduced to 50% in the 12-well format in comparison to the 6-well format.

14

#### 15 **4. Extracellular luminal and abluminal U concentrations**

16 Despite there being no modification of the BBB permeability, the extracellular concentration  
17 results showed that U was capable of accessing the abluminal side from 1 h of exposure in both types  
18 of culture (models A & B). Only three conditions were analyzed for the quantification of extracellular  
19 U between both compartments (abluminal and luminal): 1 h, 4 h and D3D6. Mass balance (MB) was  
20 checked for every experiment and validated when it was between 65 and 135%. After 24-h exposure,  
21 the MB was not respected (around  $21.54 \pm 11.05\%$  for model A) while the non-absorbance of U in the  
22 filter and plastic and the quantification of U in cells represent less than 1% of total U added at the  
23 beginning of the exposure (*i.e.* 50  $\mu\text{M}$ ).

24 In model A, the percentage of total U in the abluminal compartment increased progressively from  
25  $54.26 \pm 17.41\%$  (1 h) to  $61.80 \pm 4.18\%$  (D3D6) and was significantly different ( $p < 0.05$ ) in D3D6  
26 conditions in comparison with culture exposed for 1 h (**Figure 5**). In model B, the same tendency was

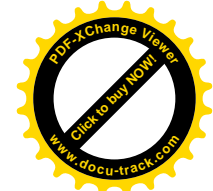


1 observed and the luminal and abluminal compartments in D3D6 conditions were statistically different  
2 (p<0.001) from 1-h exposure. Nevertheless, there were some differences between models A and B  
3 regarding the percentage of total U detected at the end of the experiment. After 1-h exposure, there  
4 was a statistically higher quantity in the luminal compartment in model B (x 1.6 times, 86.14 ±  
5 12.82%) than in model A (p<0.001). Inversely, there was statistically less in the abluminal  
6 compartment in model B (16.96 ± 12.24%) than in model A (x 2.7 times, 45.74 ± 17.41%) (p<0.001).  
7 After 4- and 72-h exposure, in model B, the presence of pericytes had not significantly modified U  
8 passage through the cells.

## 10 5. Intracellular localization of U by microscopical analyses

11 Using ICP MS analysis, U was quantified inside each type of cell and represented only 1% of added  
12 mass at the beginning of the experiment (data not shown). In order to identify U localization,  
13 transmission electronic microscopy (TEM) analyses were performed in control conditions and after  
14 different times of U exposure. In controls, one or two layers of hCMEC/D3 cells were detected with  
15 no signs of damage: TJ, endosomal activity and vesicles with multilamellar/multivesicular/cottony-  
16 like bodies were detected. After U exposure, TJ were always detected as correlated with the LY  
17 permeability results (**Figure 4**). To distinguish the different types of cells in model B, we  
18 characterized the presence of pericytes in one side of the filter by extensive granular endoplasmic  
19 reticulum. Interestingly, electron-dense needle-like structures were detected from 1 h of exposure, but  
20 were not observed in both cell types. After 1 h of exposure, these urchin-shaped precipitates were  
21 detected only in hCMEC/D3 cells in models A and B (**Error! Reference source not found.C & D**).  
22 They were localized between the cells and the filter, between the cells and, more rarely, on the luminal  
23 side of these cells (**Figure 6E & F, Figure 7D & E**). The structures were localized also inside the  
24 cells, mainly in the multilamellar/multivesicular vesicles and sometimes in structures without lipid  
25 membrane (**Figure 7A & B**). Unexpectedly, these structures were not found in pericytes, and after  
26 other times of exposure. Analytical microscopy by TEM/STEM-EDX was performed on several



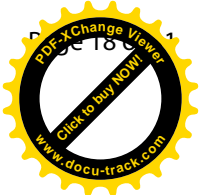
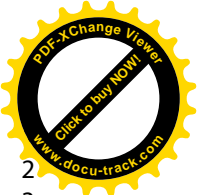


1 electron-dense needle-like structures detected inside or outside the cells to confirm the presence of U.  
2  
3  
4  
5 2 U formed fine plate-like structures that were isolated or grouped in urchin-shaped precipitates reaching  
6  
7 3 150 nm in diameter (**Figure 7B & C, E & F**).  
8  
9

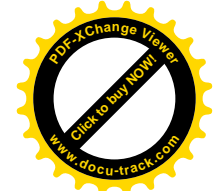
#### 10 4 11 12 13 **DISCUSSION:** 14

15 6 U is an emerging environmental pollutant and its neurological effects were described after exposure in  
16  
17 7 human and rodent models (Dinocourt et al. 2015). The quantity of U detected in the brain is low and  
18  
19 8 heterogeneous (Houpert et al. 2005; Houpert et al. 2007) and the mechanism of U transfer into the  
20  
21 9 brain remains unclear. The BBB regulates the access of endogenous and exogenous molecules (Weiss  
22  
23 10 et al. 2009) and its impairment could be involved in behavioral effects (Obermeier et al. 2013). Thanks  
24  
25 11 to human mono- and co-culture *in vitro* models, we have shed light on the effects of U after different  
26  
27 12 time exposures on paracellular permeability, extracellular concentration of U and its intracellular  
28  
29 13 localization.  
30  
31

32  
33 14 The cytotoxicity of U was studied in hCMEC/D3 cell lines and human primary pericytes (HBBP). No  
34  
35 15 toxic effect was observed in either type of cell until 500  $\mu\text{M}$  after 24 h of exposure. There are studies  
36  
37 16 with U in rat lung epithelial cells that indicate a dose-dependent cytotoxicity, with a significant  
38  
39 17 decrease in cell viability after 72 h of exposure to 500  $\mu\text{M}$  (Periyakaruppan et al. 2007). In renal  
40  
41 18 epithelial cells, viability was reduced by 20% at 500  $\mu\text{M}$  and there was minimal alteration at 250  $\mu\text{M}$   
42  
43 19 after 24-h exposure (Carrière 2015). Recently, Pierrefite-Carle et al. reported 50% loss of viability  
44  
45 20 around 390  $\mu\text{M}$  in an osteosarcoma cell line (Pierrefite-Carle et al. 2017). There is only one report on  
46  
47 21 rat brain endothelial cells that found no toxic effects at 10 and 50  $\mu\text{M}$  both for 3 and 6 h of exposure  
48  
49 22 (Dobson AW et al. 2006). Furthermore, despite the fact that cytotoxic tests of U have never been  
50  
51 23 performed in human endothelium and pericytes, all of these studies support the fact that short-term  
52  
53 24 exposure does not cause any visible effects on the cell's viability until relatively high concentrations,  
54  
55 25 namely 500  $\mu\text{M}$ .  
56  
57  
58  
59  
60



2  
3 1 Pericytes are contractile smooth muscle-like cells that cover the abluminal surface of microvessels.  
4  
5 2 They make contact with endothelial cells by holes in the basal lamina (BL) and by extensions that  
6  
7 3 cover 20 to 30% of the vascular circumference. In the present study, primary cells isolated from  
8  
9 4 human brain were used, which are easily available and have been previously used *in vitro* (Stratman et  
10  
11 5 al. 2009; Hatherell et al. 2011). Pericytes were cultivated under the filter to mimic the NVU  
12  
13 6 organization. There are several reports of co-culture models of endothelial cells (ECs) and pericytes,  
14  
15 7 but the influence of pericytes depends on the *in vitro* models. In rat and mouse models,  
16  
17 8 transendothelial electrical resistance (TEER) increased in brain endothelial cells (Nakagawa et al.  
18  
19 9 2007; Daneman et al. 2010), whereas, in pig models, it was reduced in co-culture with pericytes due to  
20  
21 10 an induction of MMPs (Zozulya et al. 2008). In our study, the paracellular Pe was increased in co-  
22  
23 11 culture with pericytes in comparison to monoculture. This was not in agreement with the increase of  
24  
25 12 TEER observed by Hatherell and coworkers in co-culture of hCMEC/D3 cells and HBPV (Hatherell et  
26  
27 13 al. 2011). On the one hand, *in vitro*, the differentiation state of pericytes could influence the TEER  
28  
29 14 (Thanabalasundaram et al. 2011). On the other hand, *in vivo*, pericytes do not have an effect on TJ  
30  
31 15 protein expression, but decrease expression of the genes involved by favoring vascular permeability  
32  
33 16 (Daneman et al. 2010). Regardless of the permeability marker, the pericytes' effects remain unclear  
34  
35 17 and it is difficult to state whether there is a beneficial effect of co-culture with HBPV in this model.  
36  
37  
38  
39  
40 18 No effect of the different times of exposure to U was observed on the paracellular Pe in these two  
41  
42 19 models. The present study shows, for the first time, that the permeability of the monoculture of human  
43  
44 20 cerebral microvascular endothelial cells is not disturbed by U after acute or chronic exposure. The  
45  
46 21 extracellular concentration of U was assayed and our results show that U is able to reach the abluminal  
47  
48 22 compartment, here mimicking the cerebral area in both mono- and co-culture models. U passage was  
49  
50 23 detected from 1 h of exposure and the rate of passage was progressive until 72 h of exposure, when  
51  
52 24 equilibrium was reached. Interestingly, there were significant differences between the two models  
53  
54 25 after 1 h of exposure. The U content in the luminal compartment was higher in co-culture models than  
55  
56 26 in monoculture models. Despite the increased permeability of the monoculture of hCMEC/D3 cells in  
57  
58 27 the co-culture model, the extracellular concentration of U evidenced differences that were indirectly  
59  
60



1 correlated. The paracellular permeability was higher, but the U passage was reduced when pericytes  
2 were cultured under the filter. The passage was significantly slower only after 1 h of exposure, but no  
3 difference was detected for other times of exposure. This modification could be linked to the physical  
4 presence of pericytes under the filter and/or to the induction of signal pathways between ECs and  
5 pericytes.

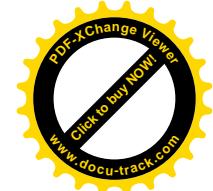
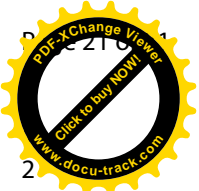
6 Therefore, it was necessary to understand how U can cross the monoculture of human cerebral  
7 microvascular endothelial cells. Transcellular passage was suggested, but paracellular passage was  
8 unfortunately not excluded because the high paracellular Pe of hCMEC/D3 cell lines can facilitate the  
9 passage of small molecules, like U, between the cells. This indicates that, only when acutely exposed,  
10 the co-culture model responds differently than the mono-culture. Therefore, pericytes seem to  
11 influence ECs rapidly since they respond differently to U exposure after 1h of exposure, but these  
12 interactions do not influence the extracellular concentration of U for longer times of exposure. The  
13 difference could also be linked to the intracellular content of each type of cell. Nevertheless, the U  
14 content represented only 1% of mass added at the beginning of the experiment in each type of cell  
15 after 1 h of exposure (data not shown). One paper states that U enters rat brain endothelial cells (RBE4  
16 cells) after only 15 minutes in the presence of 10 and 50  $\mu\text{M}$  (Dobson AW et al. 2006). The RBE4  
17 cells were cultivated in flasks, thus facilitating accumulation of U inside the cells. The use of filters  
18 prevents this artefact and permits the observation of U passage across the model. TEM and EDX  
19 analyses were performed and electron-dense needle-like structures were observed in hCMEC/D3 cell  
20 lines in mono- and co-culture after 1 h of exposure. EDX analyses confirmed the U composition of  
21 these urchin-shaped precipitates. These structures were localized in intracellular vesicles, including  
22 multilamellar and multivesicular bodies, along the endo-lysosomal pathway, among others observed in  
23 the cytoplasm. In addition, in some cases the precipitates were observed closer to the basolateral and  
24 apical side of the hCMEC/D3 cells, or outside the cells (between the cell layer and the filter). This  
25 study evidenced for the first time U precipitates in human endothelial cells. The same structures have  
26 been previously detected in renal epithelial cells and in osteoblastic cell lines (Mirto et al. 1999;  
27 Pierrefite-Carle et al. 2017). It is also well established that speciation of U influences the formation of



1 precipitates of uranyl phosphate (Mirto et al. 1999; Carriere et al. 2004). As observed in osteoblastic  
2 cell lines (Pierrefite-Carle et al. 2017), TEM analysis showed U precipitates in multivesicular bodies  
3 in endothelial cells, but not in lysosome-like vesicles, or in autophagic vesicles. Recently, Carmona et  
4 al. detected uranium in defined perinuclear regions of the cytoplasm and suggested its accumulation in  
5 organelles after exposure to SH-SY5 dopaminergic cells (Carmona et al. 2018). In the same cells,  
6 Vidaud et al. demonstrated also that urano-proteome was mainly localized in cytoplasm (Vidaud et al.  
7 2019).

8 Multi-transport could be involved in U entrance to cells. Muller and coworkers suggested that U  
9 passage is mediated mainly by absorptive endocytosis in renal cell lines, namely through sodium-  
10 dependent phosphate co-transporters (NaPi-IIas) (Muller et al. 2006). Nevertheless, these co-  
11 transporters are not expressed in brain (Hilfiker et al. 1998), but subtype III is localized in neurons,  
12 astrocytes and endothelial cells (Inden et al. 2013). The question of the entry mechanism is far from  
13 resolved, and there are many possible lines of investigation.

14 The absence of the urchin-shaped precipitates in pericytes suggests that at the beginning of the  
15 exposure, ECs stock the U as much as possible to avoid it reaching the brain. The formation of the  
16 precipitates could participate in cell detoxification process in order to protect brain parenchyma. The  
17 presence of ectopic precipitates without cytotoxicity could be explained by a very limited uranium  
18 incorporation depending on efflux and / or uptake mechanisms and intercellular variability. This  
19 observation was also suggested in neuronal cells exposed to low concentrations (Carmona et al. 2018).  
20 However, beyond their capacity to accumulate U, the cells are obliged to release it, to both the luminal  
21 and abluminal sides, allowing it to reach the brain. Furthermore, it is possible that pericytes also  
22 release U in a soluble form to the abluminal compartment, since they are also capable of uptake. The  
23 presented results support the notion that the interaction between the cell types influences the cell  
24 response when they are treated by U. Nevertheless, the observed effects of DU could be further  
25 explained by its chemical rather than radiological properties, which could influence these observed  
26 cell responses. This shows the importance of the development of new *in vitro* neurovascular unit  
27 models close to the *in vivo* structure, with addition of neuronal cells, for example.



U is known to be implicated in some neurological disorders (Dinocourt et al. 2015). Lemerrier et al. have already demonstrated that, after U perfusion, significant U content was detected in different rat brain areas, but without BBB disruption (Lemerrier et al. 2003). In previous *in vivo* model of rats chronically exposed for different times to U-contaminated drinking water, U was also detected in different brain areas (Paquet et al. 2006). To detect the impairment of BBB, S100 $\beta$  protein was analyzed in peripheral blood by immunoassay (Feriél et al. 2015). No sign of BBB disruption was observed (cf. Suppl. data). Nevertheless, interestingly, age dependence of S100 $\beta$  protein blood concentration was observed, as the highest level of S100B protein on post-natal day 21 (PND21) was seen in aged control rats ( $4.32 \pm 1.04 \mu\text{g.L}^{-1}$  for PND21 rats *versus*  $0.24 \pm 0.07 \mu\text{g.L}^{-1}$  for 6-month-old rats *versus*  $0.09 \pm 0.02 \mu\text{g.L}^{-1}$  for 9-month-old rats) (data not shown). These results are in accordance with the *in vitro* findings showing no disruption of the monoculture of hCMEC/D3 cells after U exposure.

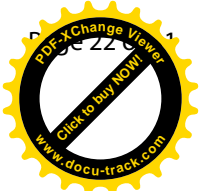
### **CONCLUSION:**

In conclusion, these results show for the first time the passage of U across the monoculture of human cerebral microvascular endothelial cells, and the intracellular localization of U precipitates without any toxicity of the barrier. Future *in vivo* studies must be conducted to elucidate translocation and retention of uranium particles into the brain and cellular and cognitive consequences in experimental animals and humans.

### **CONFLICT OF INTEREST**

None declared.

### **FUNDING INFORMATION**



2  
3  
4  
5  
6  
7  
8  
9  
10  
11  
12  
13  
14  
15  
16  
17  
18  
19  
20  
21  
22  
23  
24  
25  
26  
27  
28  
29  
30  
31  
32  
33  
34  
35  
36  
37  
38  
39  
40  
41  
42  
43  
44  
45  
46  
47  
48  
49  
50  
51  
52  
53  
54  
55  
56  
57  
58  
59  
60

1 This study was supported by the Institute for Radioprotection and Nuclear Safety (IRSN) as an  
2 Exploratory Research Project.

3

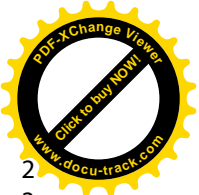
4

For Peer Review Only



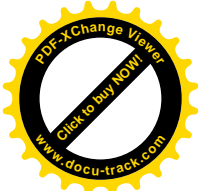
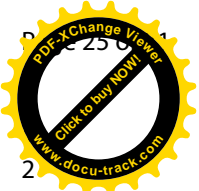
## BIBLIOGRAPHY:

- 1 Briner W, Murray J. 2005. Effects of short-term and long-term depleted uranium exposure on open-field behavior and brain lipid oxidation in rats. *Neurotoxicology and teratology*. 27(1):135-144.
- 2 Carmona A, Malard V, Avazeri E, Roudeau S, Porcaro F, Paredes E, Vidaud C, Bresson C, Ortega R. 2018. Uranium exposure of human dopaminergic cells results in low cytotoxicity, accumulation within sub-cytoplasmic regions, and down regulation of MAO-B [Research Support, Non-U.S. Gov't]. *Neurotoxicology*. 68:177-188. eng.
- 3 Carriere M, Avoscan L, Collins R, Carrot F, Khodja H, Ansoborlo E, Gouget B. 2004. Influence of uranium speciation on normal rat kidney (NRK-52E) proximal cell cytotoxicity [Comparative Study Research Support, Non-U.S. Gov't]. *Chem Res Toxicol*. 17(3):446-452. eng.
- 4 Carrière M, Gougeta, B., Galliena, J., Avoscana, L., Gobinb, R., Verbavatzb, J., Khodjaa, H. 2015. Cellular distribution of uranium after acute exposure of renal epithelial cells: SEM, TEM and nuclear microscopy analysis. *Nuclear Instruments and Methods in Physics Research Section B: Beam Interactions with Materials and Atoms*. 231(1-4):268–273.
- 5 Daneman R, Zhou L, Kebede AA, Barres BA. 2010. Pericytes are required for blood-brain barrier integrity during embryogenesis. *Nature*. 468(7323):562-566. eng.
- 6 Dang HS, Pullat VR. 1993. Normal concentration and excretion ratio of uranium in serum of normal individuals in India. *Health physics*. 65(3):303-305. eng.
- 7 Dinocourt C, Legrand M, Dublineau I, Lestaevel P. 2015. The neurotoxicology of uranium [Review]. *Toxicology*. 337:58-71. eng.
- 8 Dobson A, Lack A, Erikson K, Aschner M. 2006. Depleted uranium is not toxic to rat brain endothelial (RBE4) cells. *Biol Trace Elem Res*. 110(1):61-72. English.
- 9 Dobson AW, Lack AK, Erikson KM, Aschner M. 2006. Depleted uranium is not toxic to rat brain endothelial (RBE4) cells [Research Support, U.S. Gov't, Non-P.H.S.]. *Biological trace element research*. 110(1):61-72. eng.
- 10 Faa A, Gerosa C, Fanni D, Floris G, Eyken PV, Lachowicz JI, Nurchi VM. 2018. Depleted Uranium and Human Health [Review]. *Current medicinal chemistry*. 25(1):49-64. eng.
- 11 Ferial J, Adamo F, Monneret D, Trehel-Tursis V, Favard S, Tse C, Puybasset L, Bonnefont-Rousselot D, Imbert-Bismut F. 2015. S100B protein concentration measurement according to two different immunoassays [Letter]. *Clinical chemistry and laboratory medicine : CCLM / FESCC*. 53(7):e169-171. eng.
- 12 Gueguen Y, Suhard D, Poisson C, Manens L, Elie C, Landon G, Bouvier-Capely C, Rouas C, Benderitter M, Tessier C. 2015. Low-concentration uranium enters the HepG2 cell nucleus rapidly and induces cell stress response. *Toxicol In Vitro*. eng.
- 13 Hatherell K, Couraud PO, Romero IA, Weksler B, Pilkington GJ. 2011. Development of a three-dimensional, all-human in vitro model of the blood-brain barrier using mono-, co-, and tri-cultivation Transwell models [Research Support, Non-U.S. Gov't]. *J Neurosci Methods*. 199(2):223-229. eng.
- 14 Hilfiker H, Kvietikova I, Hartmann CM, Stange G, Murer H. 1998. Characterization of the human type II Na/Pi-cotransporter promoter [Research Support, Non-U.S. Gov't]. *Pflugers Archiv : European journal of physiology*. 436(4):591-598. eng.
- 15 Houpert P, Frelon S, Monleau M, Bussy C, Chazel V, Paquet F. 2007. Heterogeneous accumulation of uranium in the brain of rats. *Radiat Prot Dosimetry*. 127(1-4):86-89. eng.
- 16 Houpert P, Lestaevel P, Bussy C, Paquet F, Gourmelon P. 2005. Enriched but not depleted uranium affects central nervous system in long-term exposed rat. *Neurotoxicology*. 26(6):1015-1020. eng.
- 17 Inden M, Iriyama M, Takagi M, Kaneko M, Hozumi I. 2013. Localization of type-III sodium-dependent phosphate transporter 2 in the mouse brain [Research Support, Non-U.S. Gov't]. *Brain Res*. 1531:75-83. eng.
- 18 Jiang GC, Tidwell K, McLaughlin BA, Cai J, Gupta RC, Milatovic D, Nass R, Aschner M. 2007. Neurotoxic potential of depleted uranium effects in primary cortical neuron cultures and in *Caenorhabditis elegans* [Research Support, U.S. Gov't, Non-P.H.S.]. *Toxicol Sci*. 99(2):553-565. eng.



- 2  
3  
4  
5  
6  
7  
8  
9  
10  
11  
12  
13  
14  
15  
16  
17  
18  
19  
20  
21  
22  
23  
24  
25  
26  
27  
28  
29  
30  
31  
32  
33  
34  
35  
36  
37  
38  
39  
40  
41  
42  
43  
44  
45  
46  
47  
48  
49  
50  
51  
52  
53  
54  
55  
56  
57  
58  
59  
60
- 1 Keith DA, Rodriguez JP, Rodriguez-Clark KM, Nicholson E, Aapala K, Alonso A, Asmussen M, Bachman  
2 S, Basset A, Barrow EG et al. 2013. Scientific Foundations for an IUCN Red List of Ecosystems. *PLoS*  
3 *one.* 8(5):e62111. eng.  
4 Lemercier V, Millot X, Ansoborlo E, Menetrier F, Flury-Herard A, Rousselle C, Scherrmann JM. 2003.  
5 Study of uranium transfer across the blood-brain barrier. *Radiat Prot Dosimetry.* 105(1-4):243-245.  
6 eng.  
7 Lestaevel P, Dhieux B, Delissen O, Benderitter M, Aigueperse J. 2015. Uranium modifies or not  
8 behavior and antioxidant status in the hippocampus of rats exposed since birth [Research Support,  
9 Non-U.S. Gov't]. *The Journal of toxicological sciences.* 40(1):99-107. eng.  
10 Liebner S, Czapalla CJ, Wolburg H. 2011. Current concepts of blood-brain barrier development  
11 [Research Support, Non-U.S. Gov't  
12 Review]. *The International journal of developmental biology.* 55(4-5):467-476. eng.  
13 Mirto H, Barrouillet MP, Henge-Napoli MH, Ansoborlo E, Fournier M, Cambar J. 1999. Influence of  
14 uranium(VI) speciation for the evaluation of in vitro uranium cytotoxicity on LLC-PK1 cells. *Human &*  
15 *experimental toxicology.* 18(3):180-187. Eng.  
16 Muller D, Houpert P, Cambar J, Henge-Napoli MH. 2006. Role of the sodium-dependent phosphate  
17 co-transporters and of the phosphate complexes of uranyl in the cytotoxicity of uranium in LLC-PK1  
18 cells [Research Support, Non-U.S. Gov't]. *Toxicology and applied pharmacology.* 214(2):166-177. eng.  
19 Nakagawa S, Deli MA, Nakao S, Honda M, Hayashi K, Nakaoke R, Kataoka Y, Niwa M. 2007. Pericytes  
20 from brain microvessels strengthen the barrier integrity in primary cultures of rat brain endothelial  
21 cells. *Cell Mol Neurobiol.* 27(6):687-694. eng.  
22 Obermeier B, Daneman R, Ransohoff RM. 2013. Development, maintenance and disruption of the  
23 blood-brain barrier [Research Support, N.I.H., Extramural  
24 Research Support, Non-U.S. Gov't  
25 Review]. *Nature medicine.* 19(12):1584-1596. eng.  
26 Paquet F, Houpert P, Blanchardon E, Delissen O, Maubert C, Dhieux B, Moreels AM, Frelon S,  
27 Gourmelon P. 2006. Accumulation and distribution of uranium in rats after chronic exposure by  
28 ingestion. *Health Phys.* 90(2):139-147. eng.  
29 Periyakaruppan A, Kumar F, Sarkar S, Sharma CS, Ramesh GT. 2007. Uranium induces oxidative stress  
30 in lung epithelial cells [Research Support, N.I.H., Extramural  
31 Research Support, U.S. Gov't, Non-P.H.S.]. *Archives of toxicology.* 81(6):389-395. eng.  
32 Pierrefite-Carle V, Santucci-Darmanin S, Breuil V, Gritsaenko T, Vidaud C, Creff G, Solari PL, Pagnotta  
33 S, Al-Sahlane R, Auwer CD et al. 2017. Effect of natural uranium on the UMR-106 osteoblastic cell  
34 line: impairment of the autophagic process as an underlying mechanism of uranium toxicity. *Arch*  
35 *Toxicol.* 91(4):1903-1914. eng.  
36 R Software. 2016. R: A Language and Environment for Statistical Computing Version Version 1.0.136.  
37 Vienna, Austria: R Foundation for Statistical Computing.  
38 Siflinger-Birnboim A, Del Vecchio PJ, Cooper JA, Blumenstock FA, Shepard JM, Malik AB. 1987.  
39 Molecular sieving characteristics of the cultured endothelial monolayer. *Journal of cellular*  
40 *physiology.* 132(1):111-117. eng.  
41 Stratman AN, Malotte KM, Mahan RD, Davis MJ, Davis GE. 2009. Pericyte recruitment during  
42 vasculogenic tube assembly stimulates endothelial basement membrane matrix formation. *Blood.*  
43 114(24):5091-5101. eng.  
44 Thanabalasundaram G, Schneidewind J, Pieper C, Galla HJ. 2011. The impact of pericytes on the  
45 blood-brain barrier integrity depends critically on the pericyte differentiation stage. *The international*  
46 *journal of biochemistry & cell biology.* 43(9):1284-1293. eng.  
47 Tournier BB, Frelon S, Tourlonias E, Agez L, Delissen O, Dublineau I, Paquet F, Petitot F. 2009. Role of  
48 the olfactory receptor neurons in the direct transport of inhaled uranium to the rat brain [Research  
49 Support, Non-U.S. Gov't]. *Toxicol Lett.* 190(1):66-73. eng.





- 1 Vidaud C, Robert M, Paredes E, Ortega R, Avazeri E, Jing L, Guignon JM, Bresson C, Malard V. 2019.  
2 Deciphering the uranium target proteins in human dopaminergic SH-SY5Y cells. Archives of  
3 toxicology. 93(8):2141-2154. eng.  
4 Weiss N, Miller F, Cazaubon S, Couraud PO. 2009. The blood-brain barrier in brain homeostasis and  
5 neurological diseases [Review]. Biochimica et biophysica acta. 1788(4):842-857. eng.  
6 Weksler B, Romero IA, Couraud PO. 2013. The hCMEC/D3 cell line as a model of the human blood  
7 brain barrier. Fluids and barriers of the CNS. 10(1):16. eng.  
8 Weksler BB, Subileau EA, Perriere N, Charneau P, Holloway K, Leveque M, Tricoire-Leignel H, Nicotra  
9 A, Bourdoulous S, Turowski P et al. 2005. Blood-brain barrier-specific properties of a human adult  
10 brain endothelial cell line [Research Support, N.I.H., Extramural  
11 Research Support, Non-U.S. Gov't  
12 Research Support, U.S. Gov't, P.H.S.]. FASEB journal : official publication of the Federation of  
13 American Societies for Experimental Biology. 19(13):1872-1874. eng.  
14 Zeger SL, Liang KY. 1986. Longitudinal data analysis for discrete and continuous outcomes.  
15 Biometrics. 42(1):121-130. eng.  
16 Zozulya A, Weidenfeller C, Galla HJ. 2008. Pericyte-endothelial cell interaction increases MMP-9  
17 secretion at the blood-brain barrier in vitro. Brain Res. 1189:1-11. eng.

Peer Review Only



2  
3  
4  
5  
6  
7  
8  
9  
10  
11  
12  
13  
14  
15  
16  
17  
18  
19  
20  
21  
22  
23  
24  
25  
26  
27  
28  
29  
30  
31  
32  
33  
34  
35  
36  
37  
38  
39  
40  
41

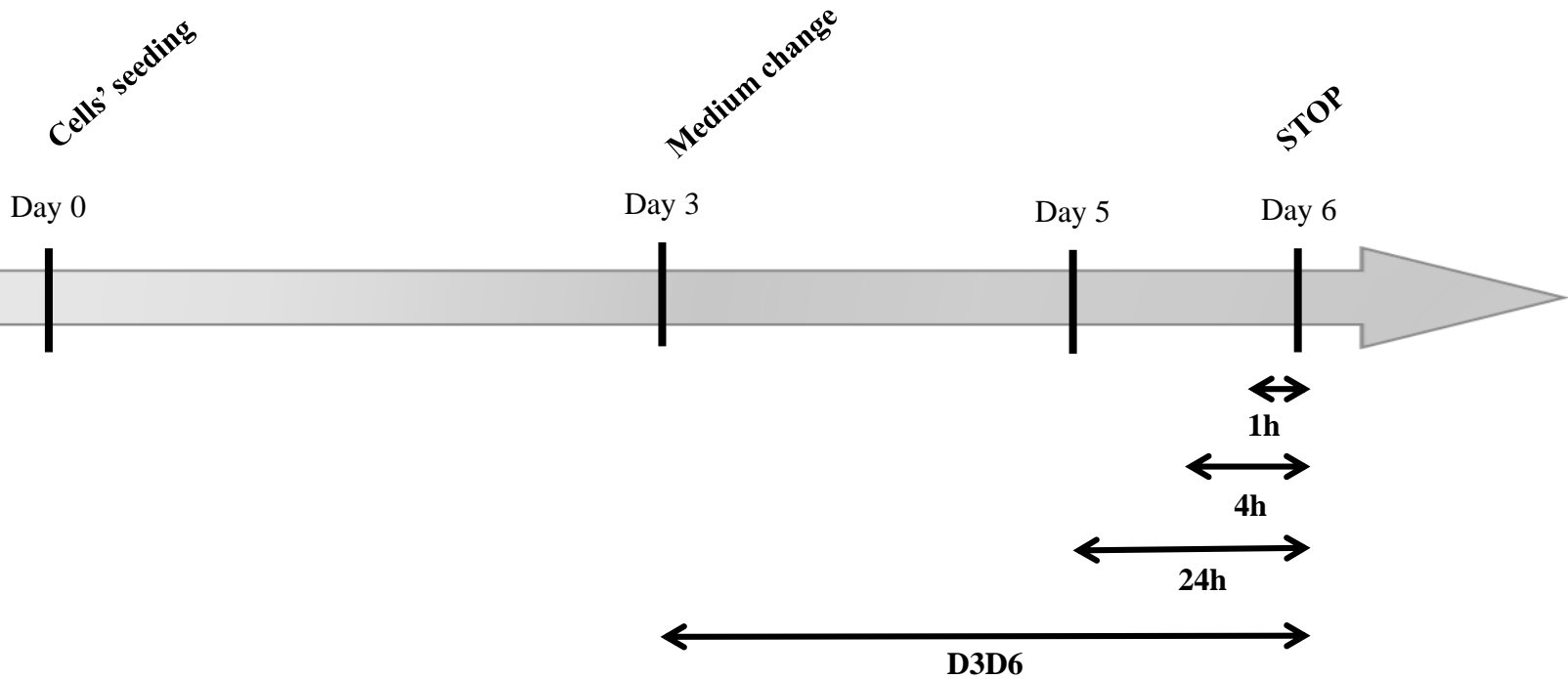


**Figure 1:** Representation of the timeline used to mimic acute and chronic exposures.

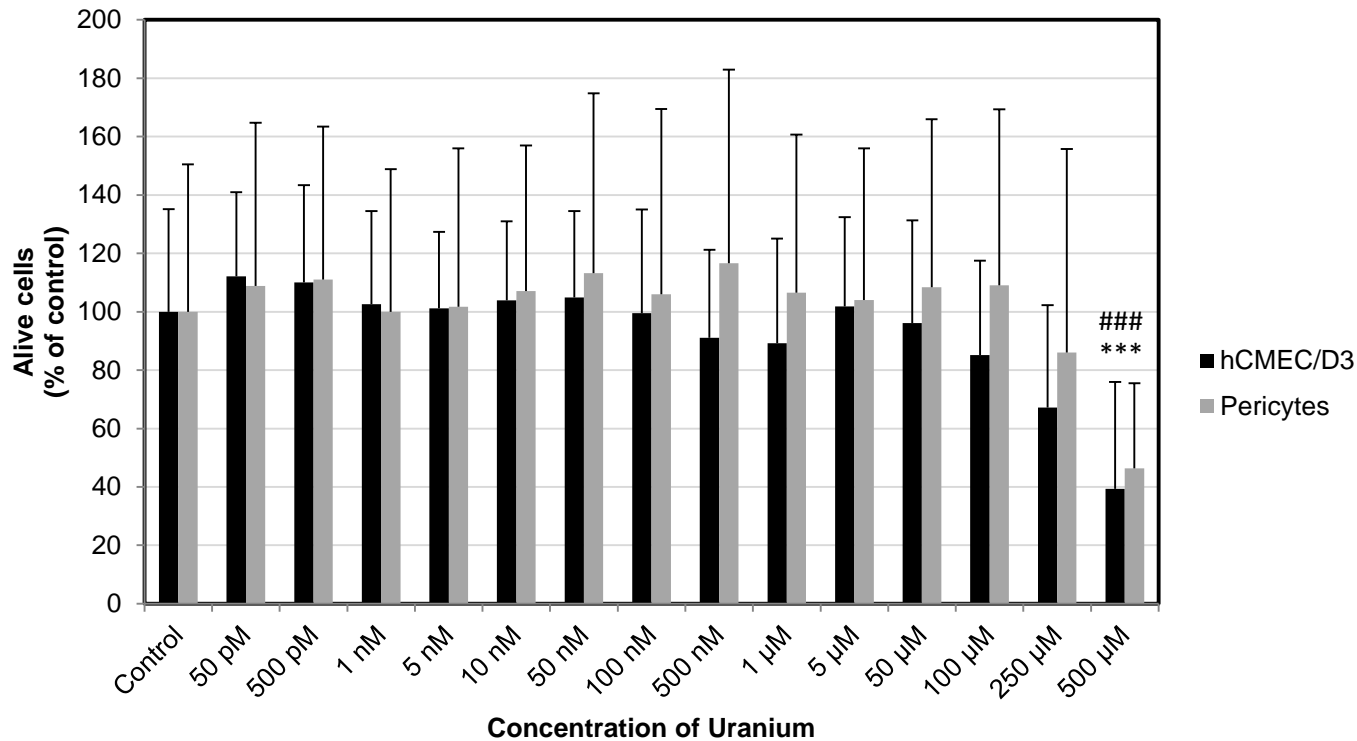


**Figure 2:** Evaluation of the cytotoxicity of 24-h exposure to U in the hCMEC/D3 cell line and in human brain pericytes by MTT assay. Results expressed as the viability of the cells normalized to the control (non-exposed cells). Mean $\pm$ SD. hCMEC/D3:\*\*\*p<0.001, Pericytes:###p<0.001. N=3 in sextuplicate.

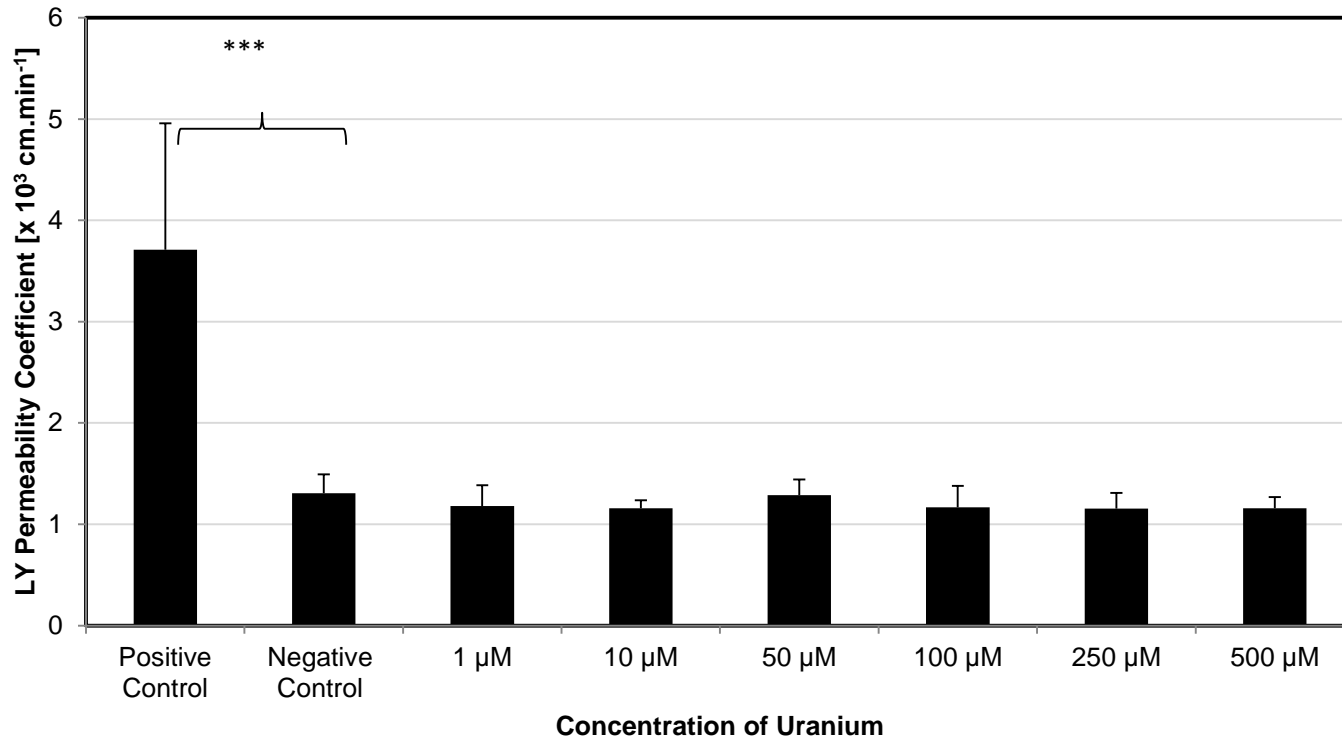


**Figure 3:** LY Permeability of hCMEC/D3 monolayer subjected to 1 to 500 μM of U at the time of the test. Results expressed as Mean±SD. \*\*\*p<0.001. N=3 in triplicate.

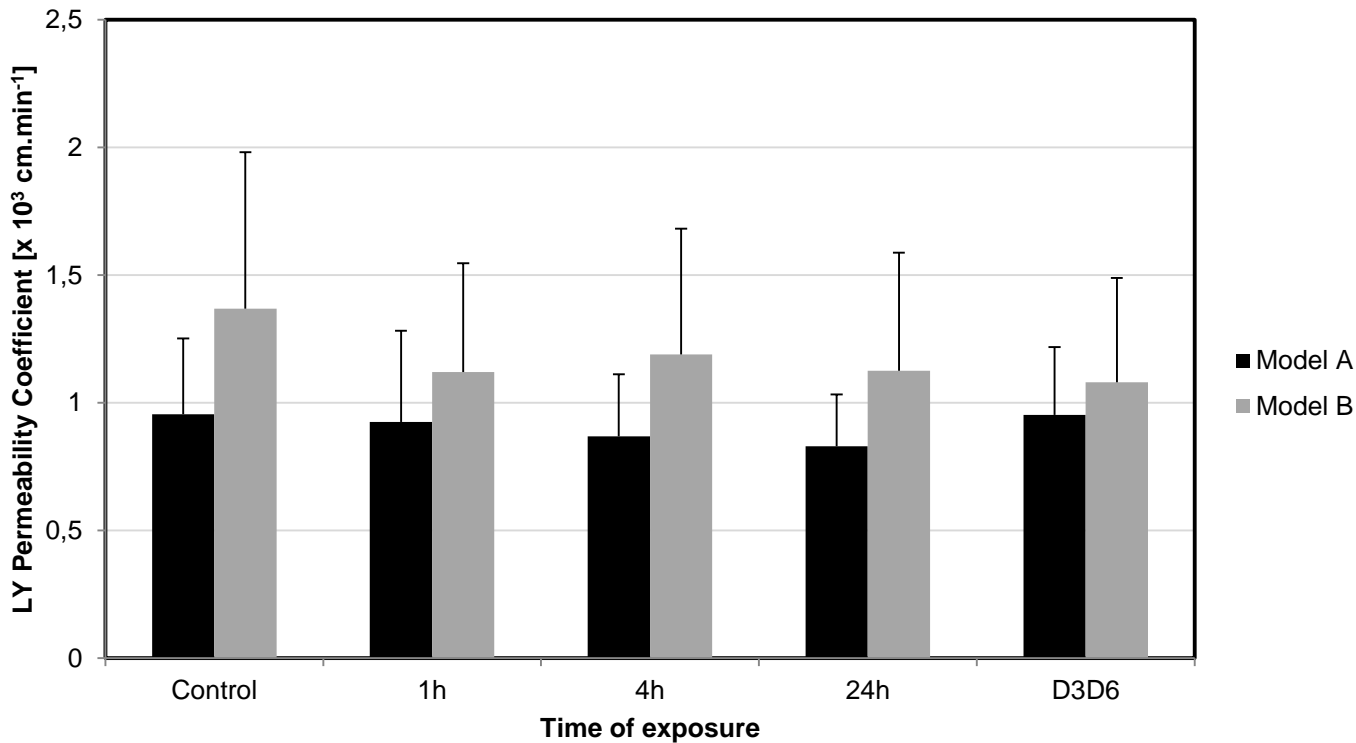


**Figure 4:** LY permeability test of model A (hCMEC/D3 cells alone) and model B (hCMEC/D3 cells and pericytes) exposed to 50  $\mu$ M U for different times. Results expressed as Mean $\pm$ SD. N=3 - 8 in triplicate.

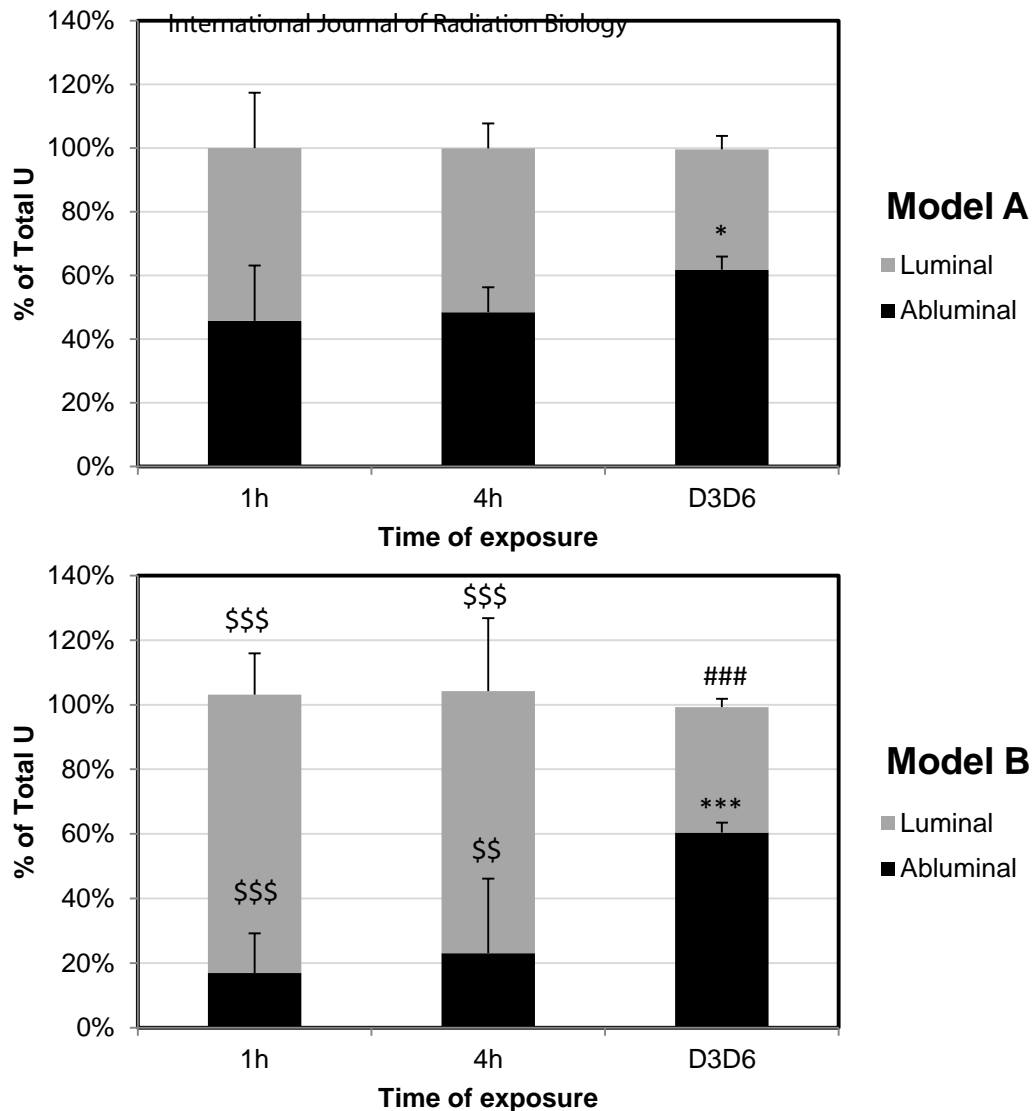
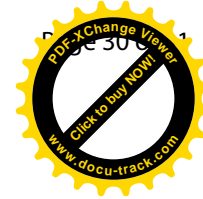
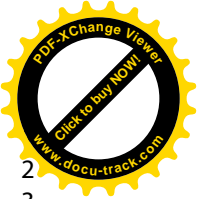
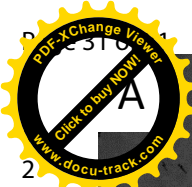
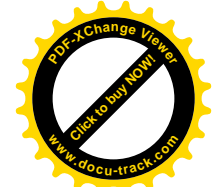


**Figure 5:** Percentage of Total U in extracellular compartments (luminal and abluminal) in model A and B exposed to 50  $\mu$ M of U for different times. Results expressed as Mean $\pm$ SD. N=3 in sextuplicate experiments. In each model, the percentage of Total U for 4 h and D3D6 conditions was compared to 1-h exposure for the luminal (\*  $p < 0.05$ , \*\*\* $p < 0.001$ ) and abluminal compartments (### $p < 0.001$ ). For each time of exposure, the percentage of Total U in each compartment was compared between model A and model B (\$\$  $p < 0.005$ , \$\$\$ $p < 0.001$ ).



# MODEL A

# MODEL B



CONTROL

1H-U exposure

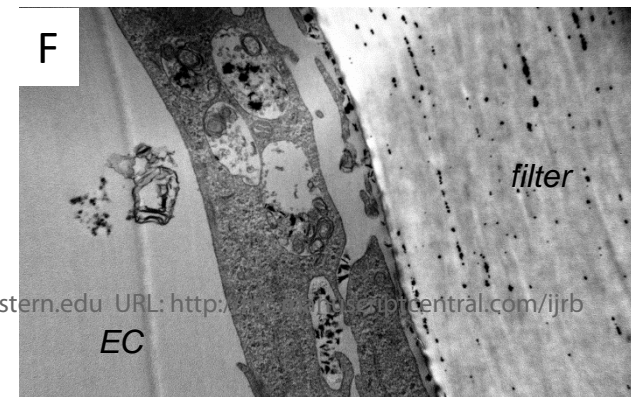
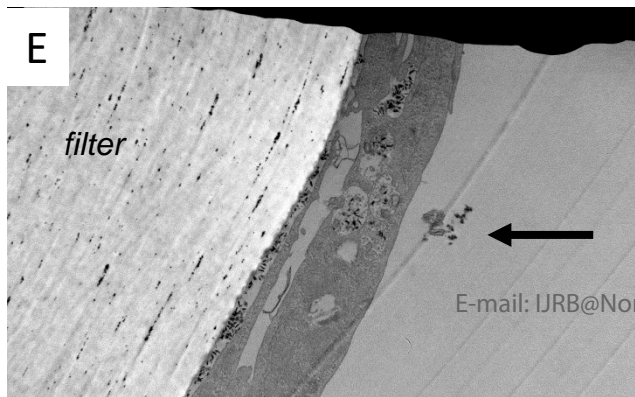
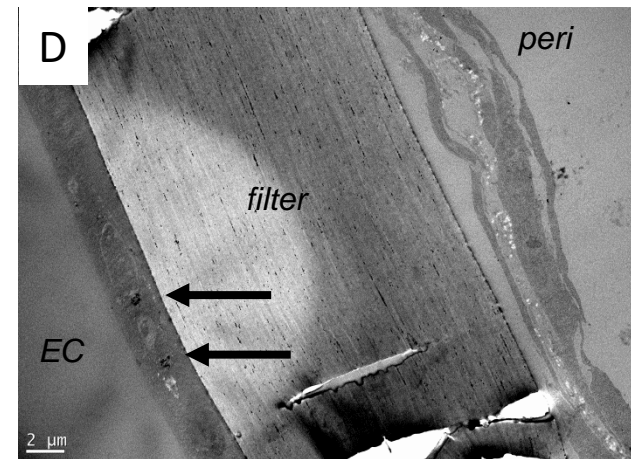
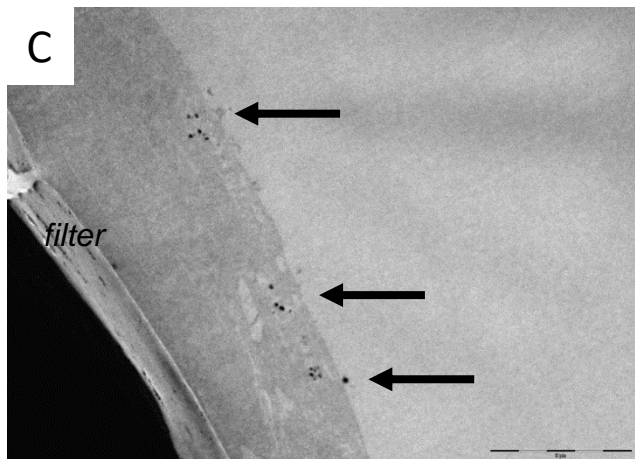
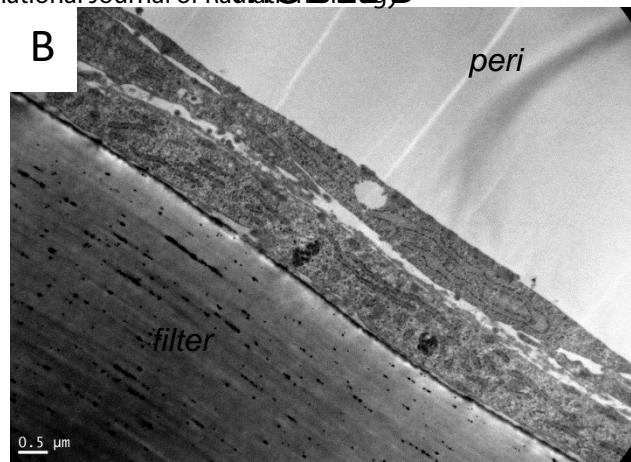
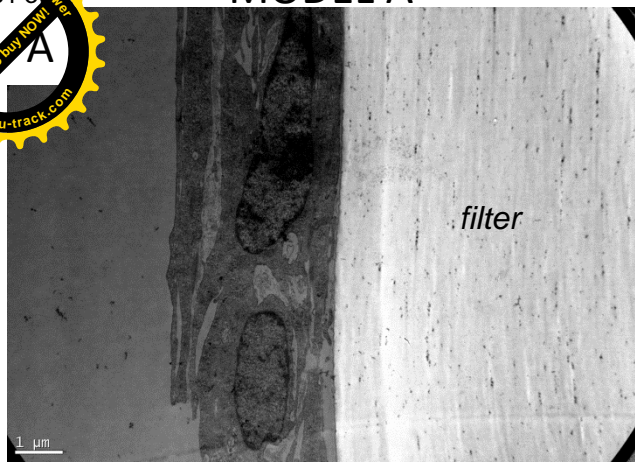


**Figure 6:** TEM ultramorphology of models A (A, C, E) and B (B, D, F): (A-B) Control, (C-F) – After 1 h of U exposure. Scales are indicated in the figure. EC: endothelial cell, Peri: pericytes. Electron-dense needle-like structures are indicated by black arrows.

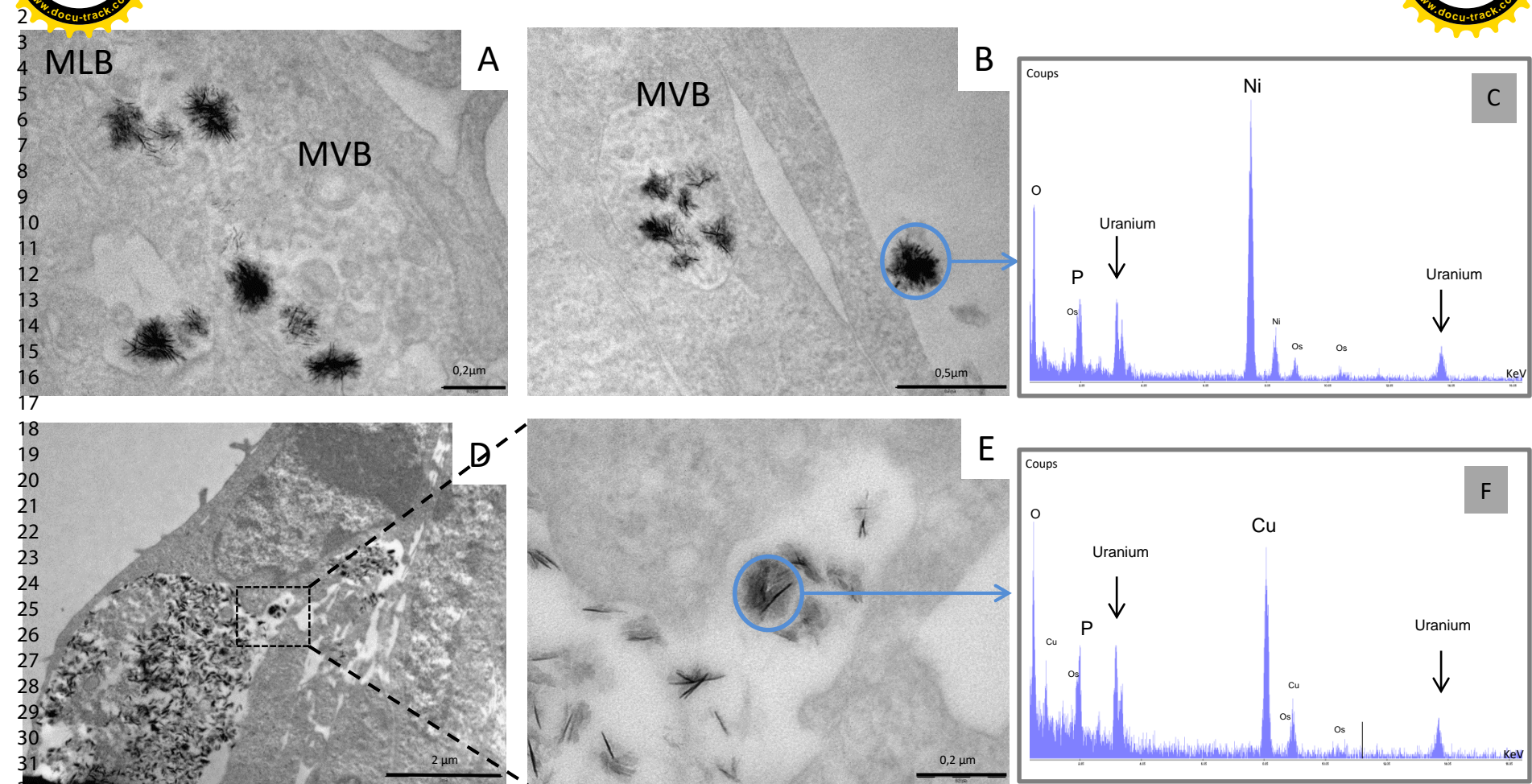
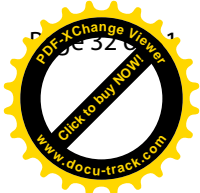
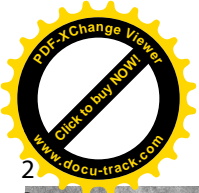


**Figure 7:** TEM/STEM-EDX observation of hCMEC/D3 cells in models A (A-B) and B (D-E) after 1 h of U exposure. MLB: multilamellar bodies, MVB: multivesicular bodies. Energy dispersive X-ray spectroscopy microanalysis of uranium-exposed models (C-F). The two highest peaks (Ni and Cu) correspond to the elements of the grids.